Probing Attosecond Dynamics by Laser Driven Electron Recollisions

J. P. Marangos[*], S. Baker[*], J. S. Robinson[*], C. A. Haworth[*], C. C. Chirila[†], M. Lein[†], L. Chipperfield[*], J. W. G. Tisch[*]

[*]*Blackett Laboratory, Imperial College, Prince Consort Road, London SW7 2BZ UK*
[†]*Institute of Physics, University of Kassel, Heinrich-Plett-Str. 40, 34132 Kassel, Germany*

Abstract. We briefly review recent advances in measurement with ~100 attosecond temporal resolution using the sub-cycle electron dynamics inherent to high order harmonic generation. In particular a technique for utilising the electron wave packet chirp is illustrated by the measurement of ultrafast proton dynamics in the H_2 molecule.

1. INTRODUCTION

The science of measurement of the time evolution of atomic and molecular processes can now claim to have entered the sub-femtosecond regime. State-of-the-art technology permits measurement of processes at a resolution approaching 100 attosecond (1 as = 10^{-18}s). The"classical" orbital periods of valence electrons in atoms are also on this timescale so it is feasible to measure atomic electron motion in real time. This breakthrough has resulted from a number of closely related techniques based around the conceptual picture of high order harmonic generation (HHG) in the strong field limit [1]. The aim of this contribution will be to describe techniques for ultra-fast measurement that are based upon our understanding of the electron dynamics driven by a laser pulse within an optical cycle. As we will show it is possible to both characterize critical parameters of the laser pulse and to measure extremely fast intra-molecular motion using these ideas.

In the strong field limit (intensity > 10^{14}Wcm^{-2}) HHG can be well understood using the semi-classical model proposed by Corkum [1][2], which separates the process into three distinct steps. Firstly, an intense linearly polarised laser pulse ionises an atom or molecule through field ionisation (predominately quantum tunnelling through the field suppressed potential barrier) when the electric field amplitude is near a peak, launching an electron wavepacket into the continuum. In the next step, the electron wavepacket moves in response to the laser field: first being accelerated away from the parent ion, and then returning at some later time (typically 0.5-1.5 fs for a laser field at 800 nm) as the laser field reverses direction. During this step the electron wavepacket gains energy from the laser field, which is then emitted as a high energy photon if recombination occurs on the return of the wavepacket to the parent ion: this is the third step in Corkum's model. The spectrum of emitted radiation extends up to a cut-off energy set by the maximum possible electron return energy which from classical considerations is $3.17U_p + I_p$ (where U_p is the ponderomotive (quiver) energy of a free

CP869, *AtomicPhysics 20, XX International Conference on Atomic Physics; ICAP 2006,*
edited by C. Roos, H. Häffner, and R. Blatt

electron in the field and I_p the ionisation potential of the state). In this strong field limit the excursion of the laser driven electron from the atom will amount to many atomic radii and so there are distinct moments within the optical cycle (see figure 1) when an electron on a given trajectory (energy) is ionised and returns.

A unique feature of this process is that under appropriate (experimenter controlled) circumstances the soft X-ray radiation is emitted with a duration much less than the optical period (2.67fs for a 800nm laser) and is exactly synchronised with the phase of the laser driving the process. A typical ultra-fast high power laser pulse might have an energy of ~1mJ and a duration of 30fs. This will be focussed into a sample of the target gas to an intensity in the range $10^{14} – 10^{15}$ Wcm^{-2}. For a central wavelength of 800nm the pulse will comprise ~10 optical cycles, therefore there are a number of cycles near the peak of the pulse that are essentially identical to each other. Harmonics are emitted within every half cycle resulting in a train of sub-femtosecond XUV pulses, separated by half the optical period, which is refered to as an attosecond pulse train or APT. Each XUV pulse has a duration given by the inverse of the available spectral bandwidth. APT's have been extensively investigated by a number of groups most notably in Lund [3][4] and Saclay [5].

The generation of an isolated, rather than a train of attosecond pulses, has also been achieved by the group of Krausz [6][7]. This is important since it allows pump-probe measurements of isolated ultra-fast events to be carried out. To do this requires laser pulses in the few-cycle limit i.e. durations ~5fs [8], such that there is only a single recollision at the highest energy the emission from which can be spectrally selected to generate the XUV pulse. An additional parameter must now be controlled which is the phase offset between the pulse envelope and the carrier wave (carrier-envelope phase –CEP); because the envelope is only a few optical cycles the CEP has a large effect upon the precise details of the field amplitude. A remarkable achievement in recent years has been the precise detection of the CEP of a pulse train and the stabilisation of this quantity, to a fixed but unknown value, in both an oscillator [9] and amplifier [10]. It is not, however, trivial to determine the absolute value of this quantity; nevertheless there is a high sensitivity of strongly non-linear processes to the CEP which makes its determination very important for attosecond science but also offers several new routes for that determination.

It is also possible to use the laser driven electron recollision in a more direct way to make attosecond domain measurements. Because the electrons return in a brief and well syncrhonised moment with an appreciable momentum (returning with kinetic energy in the 10-100eV range for typical fields) the recollision can be used as a probe in several ways. For instance Corkum and colleagues pointed out that the ionisation event forms correlated electron/nuclear wavepackets in a molecule that can be used to measure vibrational or dissociation dynamics from the kinetic energy released when the molecules are ionised by the returning electron [11]. The emission of harmonics from a molecular target of aligned molecules has been shown to carry structural information about the molecule with a very high temporal resolution [12][13][14][15][16]. This is possible because the HHG amplitude is dependent upon the dipole amplitude for the transition between the continuum state and the groundstate. As the return electron energy is in the range of 10-100eV the de Broglie wavelengths in the wavepacket span the spatial scales of interest in the groundstate

wavefunction and so the dipole is sensitive to the structure of the molecule [14]. In the strong field limit it is argued that the continuum state can be treated approximately as a superposition (wavepacket) of plane waves unaffected by the binding potential [13] and in this case the dipole matrix amplitude takes the form of a fourier transform (x-p) of the groundstate wavefunction.

Here we will be concentrate upon the temporal information that can be gained because of the unique properties of the strongly driven electrons. To understand this we must first review the laser driven electron dynamics a little more closely.

2. LASER DRIVEN ELECTRON DYNAMICS WITHIN AN OPTICAL CYCLE

To understand the basis of attosecond measurements using laser driven recollision it is necessary to examine in a little more detail the dynamics of electrons following tunnel ionisation. The tunnel ionisation occurs only near the peak of the electric field amplitude (figure 1) due to the exponential nature of the tunnelling rate [17] and so ensures that; (a) the highest energy electronic state is field ionised first, and (b) the ionization is confined in time to ~+/- 200 as (or $<1/10^{th}$ of an optical cycle). The liberated electron wavepacket moves in response to the laser field: first being accelerated away from the parent ion, and then returning some at a later time (typically 0.5-1.5 fs for a laser field at 800 nm) as the laser field reverses direction. The motion of the electron in the laser field is essentially classical motion of a charge in an oscillating electric field taking into account the constraints on the phase of the field at which the electron first appeared in the continuum and assuming that it appeared with an intial momemtum close to zero [2][18]. Only electrons tunnel ionised after the peak of the cycle may return, those arriving in the continuum before the field never receive sufficient acceleration from the field to come back and so directly ionise. During this step the electron wavepacket gains energy by virtue of the laser field up to a maximum value of $3.17U_p$ for electrons born at $1/20^{th}$ of a cycle (133 as or 300mrad after the peak). This energy is emitted as a high energy photon if recombination occurs on the return of the wavepacket to the parent ion giving the cut-off energy of $3.17U_p + I_p$.

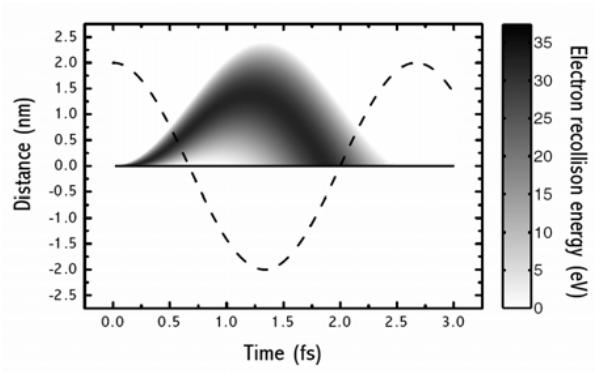

FIGURE 1. This shows the electron trajectory displacement (vertical scale) and return energy (darker = higher energy) within the trajectories launched by ionisation in the optical half-cycle peaking at t=0.0 fs. The laser electric field as a function of time is shown as a dashed line.

Electrons born into the continuum between the peak of the electric field and 1/20th of a cycle follow so called "long trajectories", travelling far from the core before the electric field reverses direction. Electrons launched into the continuum between 1/20th of a cycle and the zero-crossing of the electric field follow "short trajectories", that is, their path in the continuum is short since the electric field reverses direction relatively quickly following their birth. For electrons born at 1/20th of a cycle after the peak the short and long trajectories converge and of course this corresponds to the highest energy return and so gives rise to the highest energy photon emission (the harmonic cut-off). These groups of trajectories are illustrated in figure 1 where the electron return energy is shown using the greyscale. Within each "class" of trajectories, the energy of the colliding wavepacket varies depending on its time of birth [5][18]: e.g for electrons following shorter trajectories, those which follow the very shortest paths return with relatively low energy since they have experienced little acceleration by the field. Long trajectories have the opposite dependence with the electrons spending longer in the field returning with smaller energy. Some long trajectories give rise to multiple electron returns but their role in HHG is usually insignificant. Thus, there exists a direct relationship between the wavepacket return time, and the energy of the harmonic photon emitted: for short trajectories, successively higher orders of harmonics are generated at longer time delays. This property of HHG is fundamental to the new technique demonstrated in this work, since it allows a range of pump-probe delays to be accessed by analysis of a single harmonic spectrum.

3. HALF-CYCLE HARMONIC CUTOFFS AND CARRIER-ENVELOPE PHASE DETERMINATION

A number of methods have been demonstrated to measure the absolute value of the CEP [19][20][21] in a few-cycle laser pulse. The first, known as Stereo ATI,[20] is based on a measurement of the number of above threshold ionisation (ATI) photoelectrons ejected by atoms irradiated by the few-cycle pulse in opposite directions along the polarisation axis. A CEP dependence of asymmetry between the number of electrons detected in each direction is used to retrieve the CEP. A limitation of this technique is that it only works for pulses shorter than 8 fs (i.e. 3 cycles at a carrier wavelength of 800 nm). All of these techniques require averaging over a number of laser pulses and appear limited to pulses shorter than 8 fs (3 cycles).

For a short pulse the electric field extrema vary signicantly from one half-cycle to the next. Consequently, each half-cycle produces a spectrum with a cut-off dependent on the amplitude of the half-cycle electric-field extremum. The previous cut-off equation can thus be adapted to give an approximation of the energy of these half-cycle cut-offs (HCOs), $E_{HCO} = I_p + 3.17(E_{HCM}/2\omega)^2$ (in atomic units) where E_{HCM} is the amplitude of the half-cycle electric-field extremum. The amplitude of the half-cycle extrema are therefore mapped onto the energies of the HCOs, and thus provide detailed information about the laser pulse, in particular its CEP. It has been known for sometime that HHG is sensitive to the CEP of the laser pulse. For example, previous work has shown that the highest harmonic cutoff energy is maximised when the CEP is close to zero.

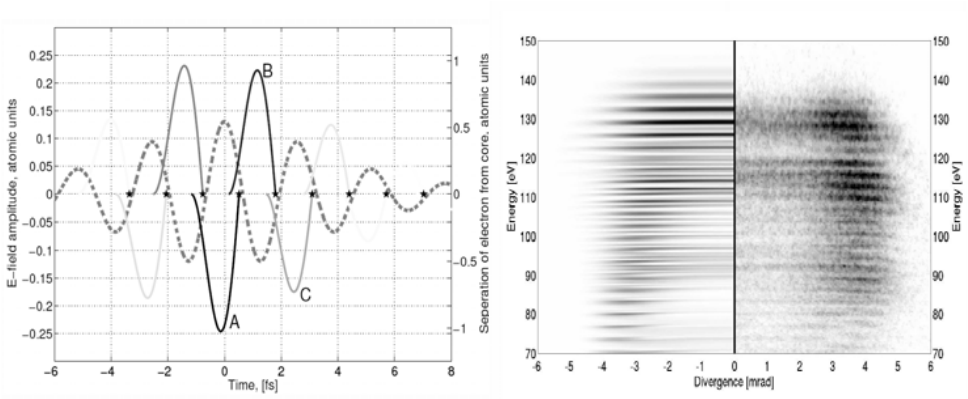

FIGURE 2. **(a)** The maximum energy trajectories (solid lines) associated with a few-cycle pulse electric field (dashed line). The larger the trajectory displacement the higher the return energy. **(b)** Spatially resolved spectra showing calculation (left frame) and measurement (right frame) for a 6 x 10^{14}Wcm^{-2} intensity 8fs pulse. Note the half-cycle cut-offs which are especially strong on axis.

We have carried out experiments to observe the infuence of CEP on HCOs in which we focus few-cycle pulses from a CEP-stabilised laser into a neon gas target to generate high harmonics. We use a set up that incorporates a spatially resolving spectrometer to record the high harmonic spectrometer. Guided by our modelling we choose phase-matching conditions which favour short electron trajectories by placing the gas target 1mm downstream of the focus. This spatially separates the HCOs to maximise their visibility. Figure 2 shows a spatially resolved HHG spectrum from Ne obtained using 8.5 fs laser pulses at a particular CEP lock value with an intensity of 6 x 10^{14}Wcm^{-2} in the interaction region. The image has been split to show the experimental data on the right hand side and the theoretical calculations on the left. The HCOs are clearly visible as lower-divergence spectral bands. We found that they wash-out in data averaged over a number of laser pulses when the CEP lock is switched off. The agreement between theory and experiment is very good. It is important to note that the HCOs are still clearly discernible in the spatially integrated data. They appear as spectral peaks that move in frequency as the CEP is changed.

Given the agreement obtained with a single-atom model, we have devised a simple algorithm that uses the positions of the the HCOs in a single HHG spectrum to retrieve the CEP of the generating laser pulse. The algorithm is capable, in principle, of a complete self-referencing retrieval of the electric field waveform of the laser pulse, including the CEP. We have tested the accuracy of the retrieval algorithm by systematically adjusting the relative CEP lock position of our phase stabilisation system, and recording the corresponding high harmonics spectra. A 50 mrad error is found for our retrieval of the CEP equivalent to measuring the field phase with a 20 attosecond resolution. The accuracy of our measurement was also tested independently of the phase stabilisation system by measuring CEP changes induced by rotating a thin (300 μm) fused silica plate in the beam at a constant CEP lock value. Our retrieved CEP matched within 100 mrad the calculated CEP slip caused by this small change in material path length.

4. CHIRP ENCODED MEASUREMENTS OF PROTON DYNAMICS IN MOLECULES

At recollision of the electron wavepacket with the parent ion the probability that recombination occurs, and therefore the strength of the harmonic signal emitted, is related to the quantum mechanical overlap between the wavefunctions of the electron wavepacket and the molecular ground state at the moment of recollision. Lein predicted [22] that the harmonic signal will be weaker from a molecule whose nuclei move quickly compared to that from a molecule with slower vibrational motion, since the overlap of the wavefunctions decreases as the internuclear separation increases. In addition, since successive orders of harmonics are generated at later times (if short electron trajectories are isolated as was the case in our experiments) [5], the ratio of the harmonic signal for instance between D_2 and H_2 should increase as the harmonic order increases. The "rate" of increase of this ratio with harmonic order then yields information concerning the differing vibrational periods of the two species, and thus represents a measurement of the nuclear motion on an attosecond timescale. We have studied HHG in gaseous H_2 and D_2 to confirm this effect, detecting a clear signature of the nuclear motion that occurs during the time interval between the ionisation and recombination steps.

The ionization step is the "pump" process in this technique, since, in the case of a molecule, a vibrational wavepacket is simultaneously launched at the moment of ionization since the nuclear state makes an instantaneous transition to the ground state potential of the molecular ion. The "probe" is the recollision of the electron wavepacket with the parent ion. This is in common with the earlier technique using correlated electron and nuclear wavepackets of Niikura et al [11]. In contrast the earlier technique used recollision induced ionisation, rather than recombination followed by emission of radiation, for the probe signal, and requires a variation of laser wavelength over a significant range in order to obtain the required pump-probe delays. In the new technique the inherent chirp in HHG emission permits a range of delays to be simultaneously measured simply by observing the harmonic spectrum.

In these experiments we chose to study the interaction with a very short laser pulse so as to isolate other processes that could be excited in a longer pulse. The intense laser field acting as the pump for HHG was provided by 8fs pulses centred at approximately 775nm. The 8fs pulses were generated by the compression of ~0.75mJ, 30fs pulses (Femtolasers CompactPRO), which had been spectrally broadened through self-phase modulation in a differentially filled, 0.25 mm inner diameter, 1m long hollow fiber. The laser beam was focused by a 400mm focal length off-axis paraboloid beneath a solenoid gas jet operating at a repetition rate of 2 Hz. The beam waist was located 9 mm before the gas jet to ensure that short electron trajectories dominated the harmonic signal. The intensity at the interaction region was estimated to be 2×10^{14} Wcm^{-2}. The harmonic signal was spectrally dispersed in a grazing incidence flat field spectrometer, and made incident upon an imaging Multi-Channel Plate (MCP) detector. The harmonic spectrum was extracted by spatial integration of the MCP image. Since the first ionization potential in the two species was very similar (15.43 eV for H_2, 15.46 eV for D_2), it was expected that the difference in phase-matching conditions for harmonic generation in the two cases is insignificant.

This was confirmed by observation that the harmonics generated in H_2 and D_2 had identical far-field spatial distributions. To make the comparison required it was essential that H_2 and D_2 were delivered to the interaction region at an equal density which was verified by an independent interferometric measurement of the particle density through full ionisation of the sample in a high power laser pulse.

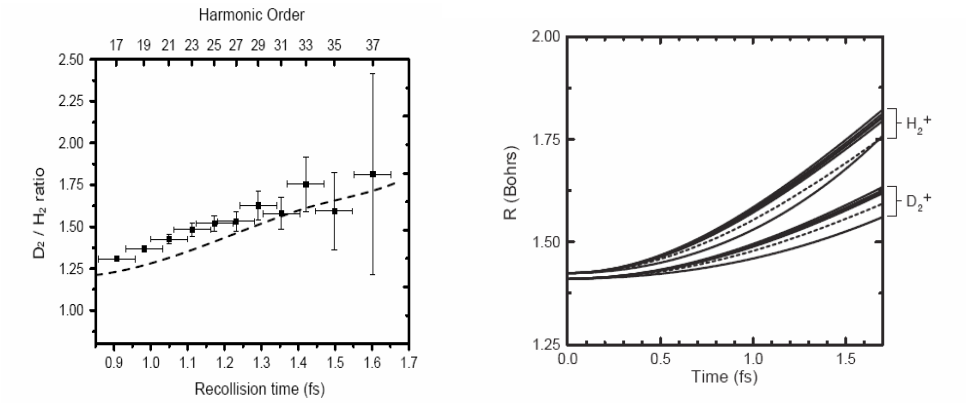

FIGURE 3. (a) Ratio of harmonic intensities for D_2/H_2 plotted as a return time (black) and a reference for the ratio of two measurements in H_2 (grey). The dashed curve is the ratio of the square of the nuclear correlation function. **(b)** Retrieved mean internuclear separation <R> as a function of time. Retrieved data from experiment using genetic algorithm (solid lines) exact calculation using potentials (dashed lines).

We compare our experimental results with a calculation based on the Strong-Field Approximation which collects the effect of the nuclear motion in the compact nuclear correlation function. The harmonics are approximately proportional to the modulus squared of the nuclear correlation function, $c(\tau) = \int \chi_0(R,0)\chi(R,\tau) f(k,R) dR$, where $\chi_0(R,0)$ and $\chi(R,\tau)$ are the initial and propagated vibrational wave packets in the molecular ion, R is the internuclear distance and τ is the travel time, which is equivalent to our delay time, Δt and f(k,R) describes the effect of two centre interference [23]. The calculated curve is scaled to account for the slight difference in photoionisation cross-sections for H_2 and D_2. We have confirmed in test calculations that the influence of the Stark shifts in the Born-Oppenheimer potential is negligible for the present set of parameters. Two-centre interference in H_2^+ (or D_2^+) gives rise to a small but clearly discernable shift which is included. As shown in Figure 3(a), we find good quantitative agreement between our measurements and the calculation.

The time evolution of the internuclear separation in each molecule was reconstructed from the recorded intensity spectra and their ratio by use of a genetic algorithm. As shown in Figure 3(b) the agreement with the exact calculation is good. Therefore, the measurement of the harmonic spectrum ratio can be used to determine proton (deuteron) motion in H_2 and D_2 molecules ~1 fs after ionisation, with a temporal resolution of ~100 as (the difference in recollision times between successive harmonic orders). Here we use the data from H_2/D_2 primarily to test and confirm the method as the potential surface and so the calculated dynamics of the proton are known in the case of H_2. Therefore the agreement between the measurement and the calculated ratio of the nuclear autocorrelation function is confirmation that the chirp of

the electron is satisfactorily given by the semi-classical treatment validating the frequency to time mapping.

5. PROSPECTS FOR FUTURE WORK AND CONCLUSIONS

The above demonstration of the measurement of the proton dynamics in a H_2^+ ion are a proof-of-principle for the chirp-encoded recollision technique. A similar experiment was conducted on CH_4^+ and revealed ultrafast rearrangement of the protons in the few femtoseconds following ionisation that take the molecule from the equilibrium tetrahedral structure of neutral CH_4 to the C_{2v} structure of the cation [23].

Further refinements of the technique are now needed. These include a fuller accounting of effects that may alter the photon energy to return time mapping e.g. Coulomb effects, two-centre interference; in principle the mapping can be checked in situ using the two-colour techniques recently reported by Dudovitch and co-workers. Extension to longer measurement times can be achieved by employing longer wavelength lasers. It should be noted the comparison of deuterated to protonated molecules of the same type was an experimental convenience that circumvented the need to more fully characterize the order dependence of the returning electron amplitude and the momentum dependent factor in the transition dipole; nevertheless this could in principle be dispensed with. For instance measuring the harmonic spectrum over a range of intensities can in principle give us the extra information needed to unravel these factors from those depending solely on the return time.

The technique should be extendable to many organic molecules containing protons the ultrafast rearrangements of which cannot be resolved by existing techniques. In principle the use of the temporal encoding of the return energy of the electrons might allow us to measure changes occurring within the states of the electrons remaining within the ion core during the “probe” electrons sojourn in the continuum. So for instance states excited by the strong field or by the removal of the electron (shake-up processes) might be time resolved with a temporal resolution of better than 100as.

ACKNOWLEDGMENTS

The authors would like to thank Peter Knight for valuable discussions. We are indebted to Peter Ruthven, Andrew Gregory and Bandu Ratanaskera for their invaluable technical support. This work was supported by the UK EPSRC and RCUK.

REFERENCES

1. P. B. Corkum, *Phys. Rev. Lett.* **71**, 1994-1997 (1993).
2. M. Lewenstein *et al., Phys. Rev. A* **49**, 2117-2132 (1994).
3. P. Antoine, A. L’Huillier and M. Lewenstein, *Phys. Rev. Lett.* **77,** 1234-1237 (1996).
4. J. Mauritsson, *Phys.Rev.Lett*. **97**, 013001 (2006)
5. Y. Mairesse *et al., Science* **302**, 1540-1543 (2003).
6. M. Drescher *et al., Science* **291**, 1923-1927 (2001).

7. R. Kienberger *et al., Nature* **427,** 817-821 (2004).
8. M. Nisoli *et al., Applied Physics B-Lasers and Optics* **65**, 189-196 (1997).
9. H. R. Telle *et al. Applied Physics B-Lasers and Optics* **69**, 327-332 (1999).
10. A. Baltuska *et al.*, *Nature* **421,** 611-615 (2003).
11. H. Niikura *et al.*, *Nature* **417**, 917-922 (2002), H. Niikura *et al. Nature* **421,** 826-829 (2003).
12. R. Velotta *et al.*, *Phys. Rev. Lett.* **87**, 183901 (2001).
13. J. Itatani *et al.*, *Nature* **432**, 867-871 (2004).
14. M. Lein, N. Hay, R. Velotta, J. P. Marangos and P. L. Knight *Phys. Rev. Lett.* **88**, 183903 (2002), M. Lein, N. Hay, Velotta, J. P. Marangos and P. L. Knight *Phys. Rev. A* **66**, 023805 (2002).
15. T. Kanai, S. Minemoto and H. Sakai, *Nature* **435**, 470-474 (2005).
16. C. Vozzi *et al.*, *Phys. Rev. Lett* **95**, 153902 (2005).
17. M. Y. Ivanov *et al.*, *J. Mod. Opt.* **52**, 165-184 (2005).
18. G. G. Paulus *et al.*, *J. Phys. B* **27**, L703-708 (1994).
19. G. G. Paulus *et al*., *Nature* **414**, 182-184 (2001).
20. A. Apolonski *et al*., *Phys. Rev. Lett.* **92**, 073902 (2004).
21. M. Kress *et al*., *Nature Physics* **2**, 327-331 (2006).
22. M. Lein, *Phys. Rev. Lett*. **94**, 053004 (2005).
23. S. Baker *et al., Science* **312**, 424-427 (2006).